Proc. Natl. Acad. Sci. USA
Vol. 89, pp. 2041–2045, March 1992
Neurobiology

Cable properties of arborized Retzius cells of the leech in culture as probed by a voltage-sensitive dye

(neurite/membrane potential/fluorescence)

PETER FROMHERZ* AND THOMAS VETTER†

Abteilung Biophysik der Universität Ulm D-7900 Ulm-Eselsberg, Federal Republic of Germany

Communicated by Erwin Neher, December 2, 1991 (received for review August 27, 1991)

ABSTRACT **Retzius cells of *Hirudo medicinalis* were cultivated on extracellular matrix protein so that extended arborizations were formed. The propagation of voltage transients along 1-μm-thick neurites was observed at a resolution of 8 μm at 10 kHz by use of a voltage-sensitive dye. Delay and width of the fluorescence transients caused by hyperpolarization of the soma are described by passive spread of voltage in a homogeneous cable (time constant, 10 ms; space constant, 320 μm). The local sensitivity of the dye was determined from a comparison of the amplitudes of fluorescence and of fitted voltage. The fluorescence transients caused by depolarization were scaled using the sensitivity profile. Action potentials were found to pervade the neurites without significant change of amplitude but with enhanced pulse width.**

An understanding of the properties of dendrites is crucial for a complete picture of neuron function. The coupling of synaptic input to neuronal output depends critically on the electrotonic characteristics and on nonlinear features of the dendritic tree (1–5). Nowadays sophisticated compartmental models based on Kelvin's cable equation may be computed with little effort. However, such computations are appropriate only if the electrical properties of a dendritic tree are known at a sufficient spatial resolution.

Hitherto the electrical properties of dendrites have been probed mainly by evaluating current–voltage relations at the soma (1, 6, 7). The method was applied, for example, to motoneurons of cat (8–12), to pyramidal neurons in the CA1 and CA3 regions of the hippocampus of guinea pig (13, 14), and to Purkinje cells of rat (15). The approach has two drawbacks: (*i*) the results are inaccurate for trees with high input impedance and (*ii*) the assignment of a cable model to a single current–voltage relation is not unique. Detailed information about the electrical properties of a dendritic tree will be attained only if it becomes possible to record the response to somatic stimulation in the dendrite itself at high spatial resolution. Voltage-sensitive dyes (16, 17) appear to be promising tools. This approach was applied to cultivated neuroblastoma cells (18), to barnacle neurons *in situ* (19), and to cultivated leech neurons (20, 21). However, the low spatial resolution and the low signal-to-noise ratio prevented a quantitative evaluation of the optical transients.

Here we report on distinctly improved optical records of voltage transients in narrow neurites of cultured Retzius cells from the central nervous system of the leech (22) with the voltage-sensitive fluorescent styryl dye RH421 (23). Resolution and signal-to-noise ratio (24) are sufficient to allow a quantitative comparison of the fluorescence transients with a simple cable model.

The publication costs of this article were defrayed in part by page charge payment. This article must therefore be hereby marked "*advertisement*" in accordance with 18 U.S.C. §1734 solely to indicate this fact.

MATERIALS AND METHODS

Neurons. Retzius cells—soma with short (primary) neurite—were dissociated from segmental ganglia of *Hirudo medicinalis* (Biopharm, Swansea, U.K.) by aspiration into a fire-polished pipette after incubation of the opened ganglia in dispase/collagenase (Boehringer Mannheim) (25). They were plated in L-15 medium (GIBCO) with 2% fetal bovine serum (GIBCO) on glass coverslips (0.15 mm thick) coated with an extract of the extracellular matrix (26), attached to silicone chambers (Flexiperm-mikro 12, Heraeus, Hanau, F.R.G.) (24). The cells were cultivated at room temperature for 2–5 days. Extended (secondary) neurites sprouted from the primary neurite. The neurons were stained with the dye RH421 (Molecular Probes) (23) by a stained-vesicle technique (24). The excitation (541 nm) and emission (>590 nm) wavelengths were optimized on the basis of the complete spectra of sensitivity of RH421 in Retzius cells (27, 28). The change of fluorescence was proportional to the voltage within a range ±70 mV around the resting potential as checked in the soma. The change was negative for depolarization.

Optical Recording. A chamber with Retzius cells was mounted on an inverted microscope (Axiomat, Zeiss) and illuminated at 541 nm by a high-pressure mercury lamp (HBO 100 W/2, Osram), an interference filter (Schott, Mainz, F.R.G.), and a shutter. The cell was projected onto an array of 100 photodiodes (each diode 1.4 mm × 1.4 mm; MD100-2; Centronics, Bristol, U.K.) in the first image plane through a ×175 objective (adapted Neofluar ×100/1.3 Oel), a dichroic beam splitter (Ft 570), and a cut-off filter (RG 590, Schott). The spatial resolution was 8 μm × 8 μm. Neuron and array were adjusted by superposing the video picture of the cell with a computer diagram of the array. Details are described in a previous paper (24). The photocurrents were fed into 100 current–voltage converters. The outputs were amplified directly or were fed into sample-and-hold amplifiers to subtract the offset of stationary fluorescence. Signals of three selected diodes were stored in a microcomputer (12 bit, 10 kHz).

The soma was impaled by a microelectrode filled with 3 M KCl (resistance 10–20 MΩ) as used in *in vivo* experiments (29). The resting potential was −40 to −55 mV. The potential was held at −50 to −55 mV to prevent spontaneous firing. Each neuron was tested 2–3 hr after application of the dye. Experiments were started only if the amplitude of the action potentials was above 60 mV.

We used two types of stimulation. (*i*) To elicit an action potential, we injected positive current into the soma. We applied a voltage of 0.1–0.4 V to the microelectrode (preresistance, 100 MΩ) for about 27 ms. (*ii*) A fast transient hyperpolarization—similar to a reversed action potential—was attained by injecting pulses of negative and positive current. A negative and a positive voltage of 3–4 V were

*To whom reprint requests should be addressed.
†Present address: Center for Biological Information Processing, Massachusetts Institute of Technology, Cambridge, MA 02139.

applied, each for 3 ms. These procedures were chosen to test the neurite in the same spectral range with respect to depolarization and hyperpolarization.

A detection site in the arborization was selected and the stationary fluorescence intensity was measured. Then the change of fluorescence was recorded during depolarizing stimulation and, after a delay of 11 ms, during hyperpolarizing stimulation. Then the record was repeated without stimulation. This reference was subtracted from the signal to eliminate effects of bleaching. The change of fluorescence was divided by the stationary fluorescence to eliminate effects of inhomogeneous illumination.

The neuritic trees were larger than the effective area of the photodiode array. We displaced the neuron relative to the array to obtain optical records from all parts of the arborization at a high resolution. To combine a set of measurements we used the peak of the membrane potential in the soma, recorded by the microelectrode, to align the records in time.

Illumination of the stained neurons resulted in a drop of the amplitude of the action potential and in an increase of width at a later stage. We restricted the number of measurements so that this photodynamic damage was negligible.

RESULTS

Transients of fluorescence in two Retzius cells of different morphology are shown in Figs. 1 and 2. In Fig. 1 a highly arborized neuron is depicted. It was depolarized and hyperpolarized by current injection into the soma.

In the first part of the experiment, an action potential was elicited. The fluorescence change was recorded in the primary neurite and in the periphery of the neuritic tree at a distance of about 350 μm. We normalized the amplitude of the peripheral transient to the amplitude of the central transient. (It is meaningless to compare the measured amplitudes because the sensitivity of the dye may change along the neuron.) The peak of the action potential was delayed by 2 ms and the half-width was enhanced from 2.5 ms to 4 ms (Fig. 1*b*). During pulse propagation various parts of the tree must be at a different potential as the delay of the pulse is comparable to its width. In the second part of the experiment, a transient hyperpolarization was induced in the soma. We scaled the peripheral fluorescence transient by the same factor used to normalize the action potential. (Thus the correction for a change of sensitivity is the same in both cases. The normalized peripheral signals may be compared in their relative amplitude.) The hyperpolarizing pulse was hardly detectable in the periphery (Fig. 1*b*). The same experiment was repeated for a second branch of the tree. Similar features of signal propagation were found there (Fig. 1*c*).

The results show that (*i*) the action potential pervades arborized neurons up to its finest processes and (*ii*) the spread of depolarization differs distinctly from the spread of hyperpolarization: it is far more efficient.

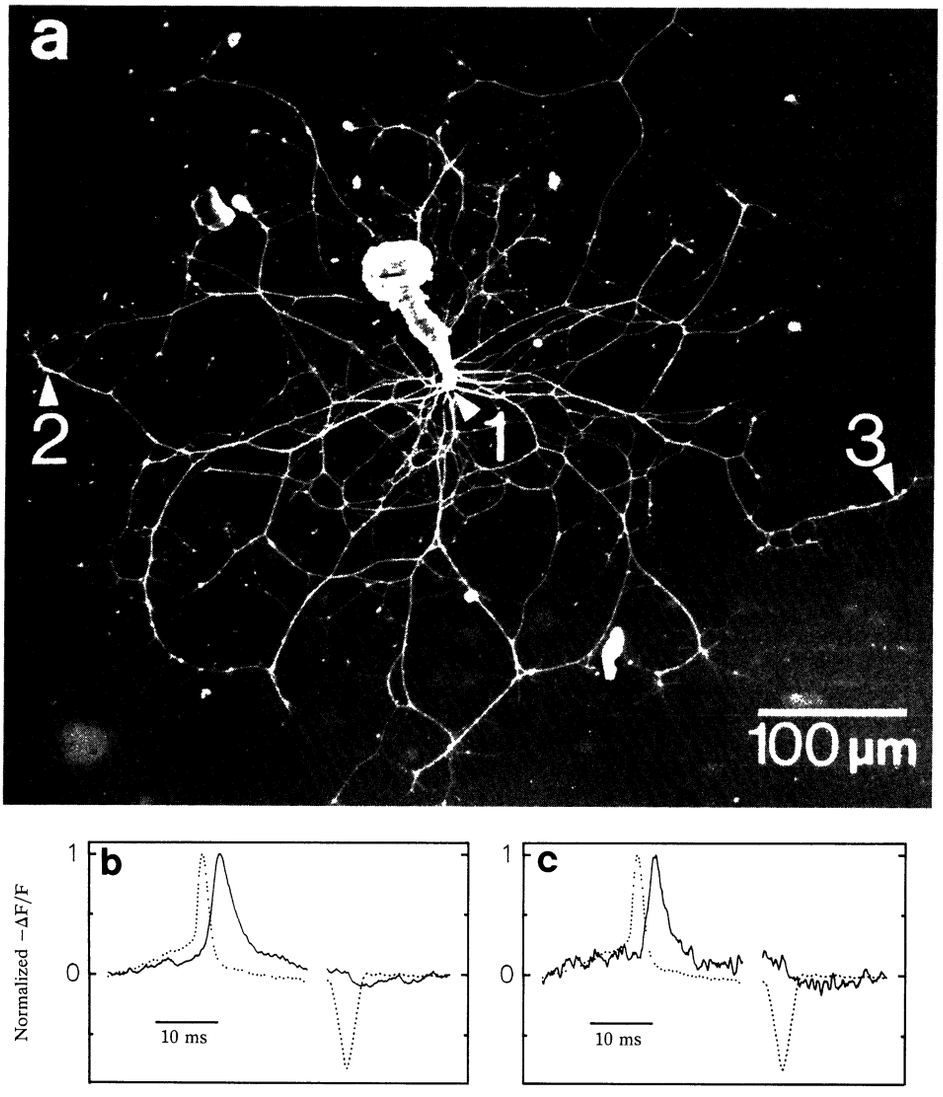

FIG. 1. Fluorescence transients in arborized Retzius cell after depolarization and hyperpolarization of the soma. (*a*) Scanning electron micrograph. Three sites of optical recording are marked. (*b* and *c*) Negative relative change of fluorescence (proportional to voltage change) vs. time for site 1 (dotted lines), site 2 (solid line in *b*), and site 3 (solid line in *c*). In the case of depolarization, amplitudes of peripheral transients are normalized to the central transient. In the case of hyperpolarization, amplitudes of peripheral signals are scaled by the same factor used to normalize the transient of depolarization. The action potential was elicited by injecting positive current for 27 ms (0.2 V at the microelectrode with 100 MΩ preresistance). The transient hyperpolarization was induced by subsequent pulses of negative and positive current each for 3 ms (±4 V at the microelectrode). Area of recording, 8 μm × 8 μm; time resolution, 10 kHz; single sweep records.

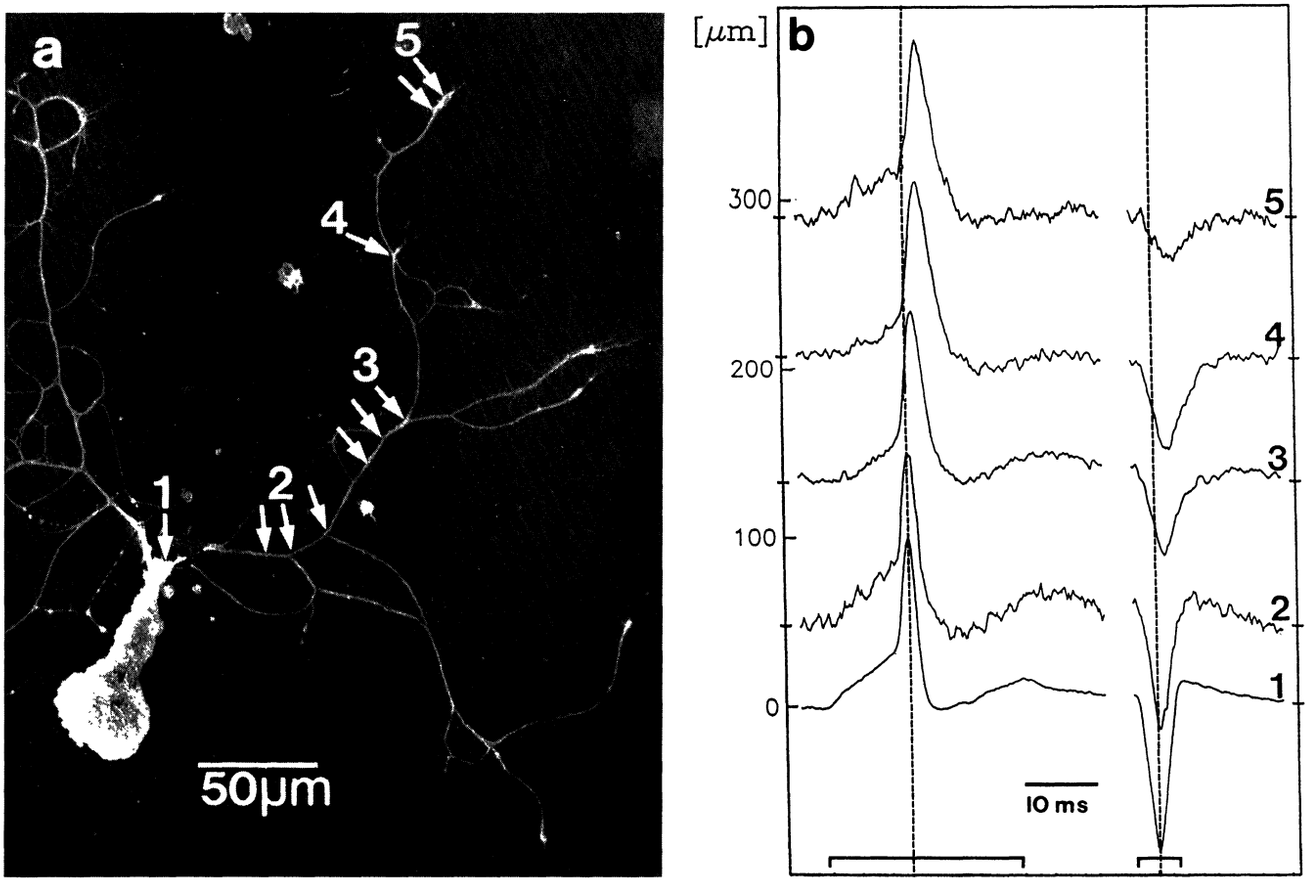

FIG. 2. Fluorescence transients in Retzius cell after depolarization and hyperpolarization of the soma. (*a*) Scanning electron micrograph. Arrows mark 10 sites of optical recording. (*b*) Negative relative change of fluorescence (proportional to voltage change) vs. time at the five sites numbered in *a*. Baselines are displaced according to the distance from the primary neurite as marked at the ordinate. Transients of depolarization are normalized in their amplitudes. Each transient of hyperpolarization is scaled by the same factor used to normalize the corresponding transient of depolarization. The action potential was elicited by injecting positive current for 27 ms (0.2 V at the microelectrode with 100 MΩ preresistance). Transient hyperpolarization was induced by subsequent pulses of negative and positive current each for 3 ms (±4 V at the microelectrode). A slight overshooting with slow relaxation was observed as the second pulse was slightly longer than the first one. Periods of stimulation are marked at the bottom. Area of recording, 8 μm × 8 μm; time resolution, 10 kHz; single sweep records.

Fig. 2 depicts a neurite with little branching. Fluorescence transients at 10 sites were recorded by applying a sequence of stimulations with the neuron being displaced with respect to the photodiode array. The soma was perturbed by transient depolarizations and hyperpolarizations as above. The fluorescence transients caused by the action potentials were normalized in their amplitudes. Five of the normalized transients are plotted on the left in Fig. 2*b*: the delay of the peak and the half-width increase continuously along the neurite. The sequence of the five records was 1, 5, 3, 2, 4. Thus the effect of delay and broadening was not due to a steady accumulation of photodynamic damage. The transients caused by hyperpolarization are shown on the right of Fig. 2*b*. At each site the fluorescence transient is scaled by the same factor used to normalize the signal of depolarization. Delay (of the peak) and half-width increase again continuously along the neurite. The relative amplitude of hyperpolarization decays. This damping is not as complete as in the highly branched neuron shown in Fig. 1.

Delay and half-width at all 10 sites marked in Fig. 2*a* are plotted in Fig. 3 for hyperpolarization and depolarization. For hyperpolarization the delay increases almost linearly with the distance. (Apparent velocity of the peak is 150 μm/ms.) The delay, as well as the enhancement of width, was rather similar in all cells studied. Data sets for two other neurons are included in Fig. 3 *a* and *b*. For depolarization we found an almost linear increase of the delay along the neurite, too. However, we observed a variability of the delay as well as of the change of width in different cells (Fig. 3 *c* and *d*). Even a reduction of pulse width was observed in an unusually thick (5–10 μm) neurite.

The relative amplitudes of the fluorescence transients are plotted in Fig. 4*a* for all 10 sites marked in Fig. 2. The profiles for hyperpolarization and for depolarization are rather irregular. We assign the irregularity to a variable effective sensitivity of the dye. (The background of fluorescence may play a crucial role: the area fraction of the diodes that detects fluorescence from neurite and from surround, respectively, is not invariant.) Such a variable local sensitivity is eliminated by division of the fluorescence signals caused by hyperpolarization and depolarization. The ratio of fluorescence transients reflects the ratio of the true voltage transients as $\Delta F_{hyp}/\Delta F_{dep} = V_{hyp}/V_{dep}$. This ratio is plotted in Fig. 4*b*. It drops rather smoothly toward the periphery studied. The decay is similar in moderately branched neurites (Fig. 4*b*) but is more pronounced in highly branched trees (see Fig. 1).

DISCUSSION

A crucial issue in the evaluation of fluorescence data of voltage-sensitive dyes is the significance of the amplitudes: the effective sensitivity of the probe is unknown and may change along the sample. We proceed in three steps. (*i*) At first we discuss width and delay time of the fluorescence transients caused by hyperpolarization without referring to

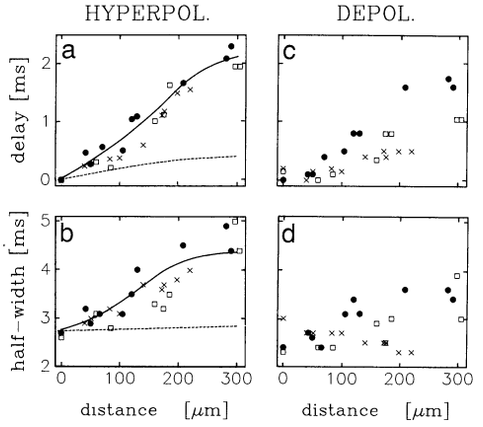

FIG. 3. Delay of peak and half-width of fluorescence transients along neurites of three Retzius cells. Filled circles refer to the neuron shown in Fig. 2. (*a*) Delay of hyperpolarization. (*b*) Half-width of hyperpolarization. (*c*) Delay of depolarization. (*d*) Half-width of depolarization. Solid lines in *a* and *b* refer to the spread of a gaussian voltage transient (initial half-width, 2.75 ms) in a homogeneous cable with sealed end (length $l = 300$ μm, diameter $d = 1$ μm, specific membrane capacitance $c_M = 1$ μF/cm^2, specific membrane conductance $g_M = 0.1$ mS/cm^2, cytoplasmic resistance $r_I = 250$ Ω·cm). Broken lines refer to spread in a cable with a lower specific resistance, $r_I = 50$ Ω·cm.

the amplitudes at all. (*ii*) Then we consider a quantitative fit of the fluorescence transients caused by hyperpolarization. From a comparison of the amplitudes of experiment and model we determine the sensitivity profile of the dye. (*iii*) Finally, we consider the propagation of the action potential by using the sensitivity profile of the dye.

To evaluate the data we use the simple model of a finite homogeneous cable driven by a voltage source at one end with an open circuit at the other (sealed) end. Such a model is equivalent to an actual tree if its geometry obeys Rall's constraints (1). These constraints are hardly satisfied by the neuron depicted in Fig. 2*a*. We use the elementary model as a help for qualitative understanding of the data in a complicated system that is incompletely characterized. [We avoid considering a compartmental cable model that accounts for the actual dimensions and the branching of the neurite. Such a model would imply necessarily a spatial variability of the electrical properties. The quality of our data is insufficient (low number and scatter of data points) to support a multiparameter fit in terms of such a detailed model.]

Passive Spread. We consider the propagation of a gaussian voltage transient of half-width 2.75 ms along a cable of diameter $d = 1$ μm and length $l = 300$ μm. Parameters are the specific capacitance c_M and conductance g_M of the membrane and the specific resistance r_I of the cytoplasm. We define the time constant $\tau = c_M/g_M$, the length constant $\lambda = \sqrt{d/4 \cdot r_I g_M}$, and the propagation constant $D = \lambda^2/\tau = d/4 \cdot r_I c_M$. The polarization $V(x, t)$ (the difference between membrane potential and resting potential as a function of space and time) is evaluated by integration of the cable equation $\partial_t V = D\partial_{xx} V - V/\tau$. For standard values $c_M = 1$ μF/cm^2, $g_M = 0.1$ mS/cm^2, and $r_I = 50$ Ω·cm (30), we obtain $\tau = 10$ ms, $\lambda = 710$ μm, and $D = 0.5$ cm^2/s. The computed values of the delay of the peak and of the half-width are plotted in Fig. 3 *a* and *b*. Both the delay and the change of width are distinctly smaller than observed. A change of τ has little effect on delay and broadening. By choosing a lower propagation constant, $D = 0.1$ cm^2/s (i.e., shorter length constant, $\lambda = 320$ μm), however, we compute delays and half-widths which are similar to the experimental data (Fig. 3 *a* and *b*). In particular, the model describes the almost linear increase of the delay with the distance.

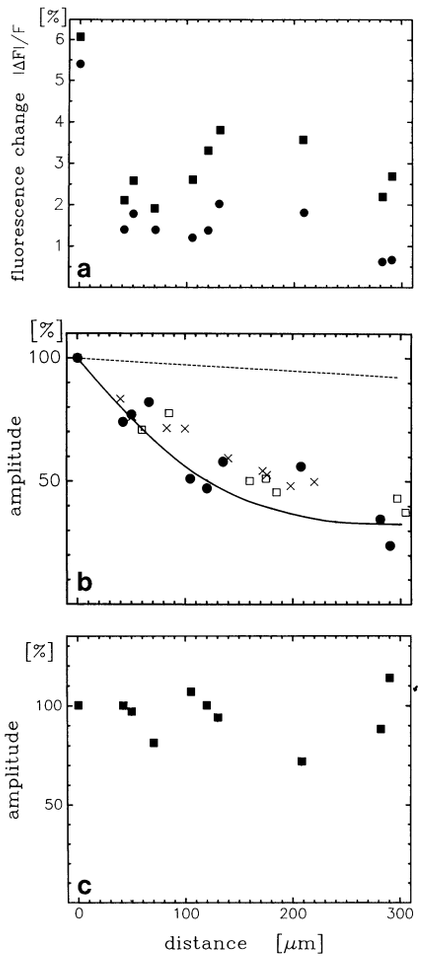

FIG. 4. Amplitude of fluorescence transients along neurites of Retzius cells. Filled symbols refer to the neuron shown in Fig. 2. (*a*) Absolute value of the amplitude of relative fluorescence. ■, Depolarization; ●, hyperpolarization. (*b*) Ratio of the relative fluorescence amplitudes for hyperpolarization and depolarization scaled to 100% for the signal in the primary neurite. Solid line refers to spread of a gaussian voltage transient (initial half-width, 2.75 ms) in a homogeneous cable with sealed end (length $l = 300$ μm, diameter $d = 1$ μm, specific membrane capacitance $c_M = 1$ μF/cm^2, specific membrane conductance $g_M = 0.1$ mS/cm^2, cytoplasmic resistance $r_I = 250$ Ω·cm). Broken line refers to spread in such a cable with a lower cytoplasmic resistance, $r_I = 50$ Ω·cm. (*c*) Amplitudes of depolarization scaled by the relative local sensitivities of the dye.

The calculated amplitudes are drawn in Fig. 4*b*. In the case of low D, the amplitude follows nicely the ratio of the fluorescence amplitudes, $\Delta F_{hyp}/\Delta F_{dep}$. The coincidence of computed V_{hyp} and measured $\Delta F_{hyp}/\Delta F_{dep} = V_{hyp}/V_{dep}$ is compatible with the assumption that the amplitude of the depolarization is rather invariant.

The value of $D = 0.1$ cm^2/s corresponds to a cytoplasmic resistance $r_I = 250$ Ω·cm at diameter $d = 1$ μm and capacitance $c_M = 1$ μF/cm^2. It is similar to the value $r_I = 225$ Ω·cm assigned to Purkinje cells (15) but distinctly higher than the value $r_I = 70$ Ω·cm assumed for cat motoneurons (10–12). The high cytoplasmic resistance may be due to intracellular structures (microtubules, mitochondria) that reduce the effective diameter of the neurite.

Sensitivity Profile. In a second step we evaluate the amplitudes of the fluorescence signals within the simple cable model. We compute the spread of the hyperpolarization observed at the soma. We vary time constant τ and propagation constant D and choose individual sensitivity factors at each location. Five computed voltage transients and five

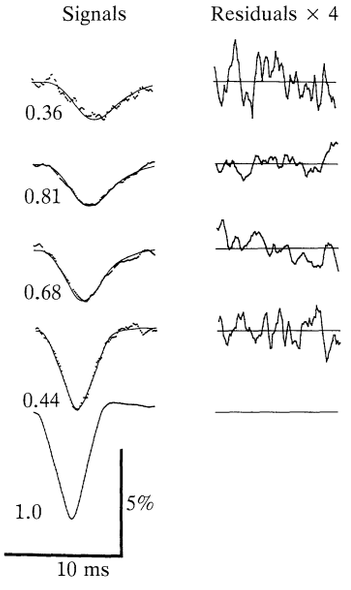

FIG. 5. Negative relative change of fluorescence at five sites along a neurite of a Retzius cell (see Fig. 2) after hyperpolarization (dotted lines in the left column). Solid lines describe the transient hyperpolarizations in a homogeneous cable with sealed end (length $l = 300$ μm) with time constant $\tau = 10$ ms and propagation constant $D = 0.1$ cm^2/s. The fluorescence transients are scaled individually to match the amplitudes of the theoretical transients. The relative sensitivities are indicated. The residuals (experiment − theory) are shown in the right column.

fluorescence transients are plotted in Fig. 5. The parameters chosen are the same as used above, $\tau = 10$ ms and $D = 0.1$ cm^2/s. The agreement of experiment and theory is almost perfect in this case, as indicated by the residuals.

The fit of the data by the cable model provides the relative voltage sensitivities of fluorescence (Fig. 5). Of course, they are valid only with respect to the simple model used: irregularities of the tree (branch points, electrical inhomogeneities) are attributed implicitly to the sensitivity profile.

We assign the irregular profile of the fluorescence amplitudes of hyperpolarization (Fig. 4*a*) to the superposition of the regular drop of the voltage amplitude (due to passive spread) and of the irregular profile of sensitivity.

Action Potential. Finally we calibrate the amplitudes of the fluorescence transients caused by depolarization (Fig. 4*a*), by using the relative sensitivities evaluated from hyperpolarization as indicated in Fig. 5. These calibrated amplitudes are plotted in Fig. 4*c*. Within the experimental error we find that the action potential propagates at invariant amplitude from the soma to the tips of the neuritic tree. Thus the normalized fluorescence transients depicted in Fig. 2 reflect the actual voltage transients adequately.

The undamped propagation of depolarization is quite different from passive spread. With its enhanced width, it differs also from a Hodgkin–Huxley type of propagation in a homogeneous cable with invariant width and amplitude (31). An inhomogeneous distribution of channels may provide a simple interpretation for a propagation at constant amplitude but changed width. Numerical solutions of the Hodgkin–Huxley equation show, for example, that a reduction of K^+ conductance along the cable gives rise to broadening. Also, the observation of a narrowed action potential (Fig. 3*d*) may be discussed within such a context. Numerical simulations indicate that changes of geometry play a minor role.

Conclusions. We recorded electrical transients in neurites of cultivated Retzius cells at a high spatiotemporal resolution by using a voltage-sensitive dye. The resolution was sufficient to allow an evaluation by a simple cable model. The propagation of hyperpolarization was attributed to passive spread. On the basis of this assignment we determined the profile of sensitivity of the probe. Using this calibration we found that action potentials pervaded the neuritic tree without significant damping. Such information may be difficult to obtain by conventional electrophysiological methods.

A straightforward generalization of the results is not possible—i.e., the electrical features of cultivated Retzius cells cannot be attributed to Retzius cells *in vivo* or to other central neurons of invertebrates and vertebrates. Nonetheless, the experimental data on the electrotonic features of narrow neurites and on the propagation of the action potential in a neuritic tree may be useful in the discussion of dendritic integration—i.e., with respect to the effect of dendritic synapses on spike generation near the soma and to the effect of spikes invading the dendritic tree.

The present paper provides no final characterization of signal propagation in an arborized neuron. However, it points out the direction to go in order to take full advantage of the method of voltage-sensitive dyes. To obtain a complete electrical description of axonal or dendritic trees, we shall have to fit fluorescence transients on the basis of a compartmental cable model that accounts for the geometry of a tree and for variations of the local properties of the cable. Such an approach will be possible with the use of a larger number of detection sites at higher spatial resolution, improved dyes (28), and arborizations of designed geometry (32).

This project was supported by the Deutsche Forschungsgemeinschaft (Grant Fr349/5) and by the Land Baden-Württemberg (Forschungsschwerpunkt 24).

1. Rall, W. (1959) *Exp. Neurol.* **1,** 491–527.
2. Traub, R. D. & Llinas, R. (1979) *J. Neurophysiol.* **42,** 476–496.
3. Koch, C., Poggio, T. & Torre, V. (1982) *Philos. Trans. R. Soc. London Ser. B* **298,** 227–264.
4. Hounsgaard, J. & Midtgaard, J. (1989) *Trends Neurosci.* **12,** 313–315.
5. Llinas, R. R. (1989) *Science* **242,** 1613–1632.
6. Rall, W. (1960) *Exp. Neurol.* **2,** 503–532.
7. Rall, W. (1969) *Biophys. J.* **9,** 1483–1508.
8. Lux, H. D. & Pollen, D. A. (1966) *J. Neurophysiol.* **29,** 207–220.
9. Nelson, P. G. & Lux, H. D. (1970) *Biophys. J.* **10,** 55–73.
10. Barrett, J. N. & Crill, W. E. (1974) *J. Physiol. (London)* **239,** 301–324.
11. Fleshman, J. W., Segev, I. & Burke, R. E. (1988) *J. Neurophysiol.* **60,** 60–85.
12. Clement, J. D. & Redman, S. J. (1989) *J. Physiol. (London)* **409,** 63–87.
13. Brown, T. H., Fricke, R. A. & Perkel, D. H. (1981) *J. Neurophysiol.* **46,** 812–827.
14. Turner, D. A. (1984) *Biophys. J.* **46,** 73–84.
15. Shelton, D. P. (1985) *Neuroscience* **14,** 111–131.
16. Salzberg, B. M., Davila, H. V. & Cohen, L. B. (1973) *Nature (London)* **246,** 508–509.
17. Cohen, L. B. & Lesher, S. (1986) in *Optical Methods in Cell Physiology*, eds. de Weer, P. & Salzberg, B. M. (Wiley, New York), pp. 72–99.
18. Grinvald, A., Ross, W. N. & Farber, I. C. (1981) *Proc. Natl. Acad. Sci. USA* **78,** 3245–3249.
19. Krauthamer, V. & Ross, W. N. (1984) *J. Neurosci.* **4,** 673–682.
20. Ross, W. N., Arechiga, H. & Nicholls, J. G. (1987) *J. Neurosci.* **7,** 3877–3887.
21. Ross, W. N., Arechiga, H. & Nicholls, J. G. (1988) *Proc. Natl. Acad. Sci. USA* **85,** 4075–4078.
22. Chiquet, M. & Nicholls, J. G. (1987) *J. Exp. Biol.* **132,** 191–206.
23. Grinvald, A., Fine, I., Farber, I. C. & Hildesheim, R. (1983) *Biophys. J.* **42,** 195–198.
24. Fromherz, P. & Vetter, T. (1991) *Z. Naturforsch. C* **46,** 687–696.
25. Dietzel, I. D., Drapeau, P. & Nicholls, J. G. (1986) *J. Physiol. (London)* **372,** 191–205.
26. Chiquet, M., Masude-Nakagawa, L. & Beck, K. (1988) *J. Cell Biol.* **107,** 1189–1198.
27. Fromherz, P. & Lambacher, A. (1991) *Biochim. Biophys. Acta* **1068,** 149–156.
28. Fromherz, P., Dambacher, K. H., Ephardt, H., Lambacher, A., Müller, C. O., Neigl, R., Schaden, H., Schenk, O. & Vetter, T. (1991) *Ber. Bunsen-Ges. Phys. Chem.* **95,** 1333–1345.
29. Nicholls, J. G. & Purves, D. (1970) *J. Physiol. (London)* **209,** 647–667.
30. Katz, B. (1966) *Nerve, Muscle and Synapse* (McGraw-Hill, New York).
31. Hodgkin, A. L. & Huxley, A. F. (1952) *J. Physiol. (London)* **117,** 500–544.
32. Fromherz, P., Schaden, H. & Vetter, T. (1991) *Neurosci. Lett.* **129,** 77–80.